

Received: 2017.02.13
Accepted: 2017.05.05
Published: 2017.05.24

Fabrication and Characterization of Carbon Fiber-Reinforced Nano-Hydroxyapatite/Polyamide46 Biocomposite for Bone Substitute

Authors' Contribution:
Study Design A
Data Collection B
Statistical Analysis C
Data Interpretation D
Manuscript Preparation E
Literature Search F
Funds Collection G

ABDEF 1 **Zhennan Deng***
ABCD 2 **Hongjuan Han***
CEF 1 **Jingyuan Yang**
BC 1 **Yuanyuan Li**
BC 1 **Shengnan Du**
AFG 1 **Jianfeng Ma**

1 School and Hospital of Stomatology, Wenzhou Medical University, Wenzhou, Zhejiang, P.R. China
2 Oral Department, Sichuan Academy of Medical Sciences and Sichuan Provincial People's Hospital, Chengdu, Sichuan, P.R. China

* Co-first author (equal contribution to this work)

Corresponding Author: Jianfeng Ma, e-mail: dentmajianfeng@163.com

Source of support: Financial support provided by Scientific Research Fund of Zhejiang Provincial Education Department (Y201533871) and the Wenzhou Municipal Science and Technology Bureau Foundation of China (Y20160142)

Background: Ideal bone repair material should be of good biocompatibility and high bioactivity. Besides, their mechanical properties should be equivalent to those of natural bone. The objective of this study was to fabricate a novel biocomposite suitable for load-bearing bone defect repair.


Material/Methods: A novel biocomposite composed of carbon fiber, hydroxyapatite and polyamide46 (CF/HA/PA46) was fabricated, and its mechanical performances and preliminary cell responses were evaluated to explore its feasibility for load-bearing bone defect repair.

Results: The resultant CF/HA/PA46 biocomposite showed a bending strength of 159–223 MPa, a tensile strength of 127–199 MPa and a tensile modulus of 7.7–10.8 GPa, when the CF content was 5–20% (mass fraction) in biocomposite. The MG63 cells, showing an osteogenic phenotype, were well adhered and spread on the surface of the CF/HA/PA46 biocomposite. Moreover, the cells vitality and differentiation on the CF/HA/PA46 biocomposite surface were obviously increased during the culture time and there was no significant difference between the CF/HA/PA46 biocomposite and HA/PA (as control) at all the experimental time ($P > 0.05$).

Conclusions: The addition of CF into HA/PA46 composite manifest improved the mechanical performances and showed favorable effects on biocompatibility of MG63 cells. The obtained biocomposite has high potential for bone repair in load-bearing sites.

MeSH Keywords: **Biocompatible Materials • Compomers • Materials Testing**

Full-text PDF: <http://www.medscimonit.com/abstract/index/idArt/903768>

 3141

 2

 7

 39



Background

Ideal bone repair material should be of good biocompatibility and high bioactivity. Besides, their mechanical properties should be equivalent to or similar to those of natural bone. Nowadays, metals are mainly used of clinical application for load-bearing bone defect repair because of their flexibility and stiffness. However, due to the mismatch of the modulus between the metal implant materials and those of the natural bone, metal stress shielding on bone often result in twice trauma [1–3]. In the past few years, polymers and their composites, such as polyether ether ketone (PEEK) and reinforced PEEK by carbon fiber, ultrahigh molecular weight polyethylene (UHMWPE), nano-hydroxyapatite/polyamide66 composite (HA/PA66) have been widely studied for bone replacement due to their excellent properties [4]. Especially, among these composites, many recent studies reported that the HA/PA66 composite has good compatibility to bone and can bond directly to bone, thus it is already being widely used for spine fusion applications [5–7]. However, it is still not strong enough for load-bearing bone defect repair and fixation devices because of its shortcomings in strength and stiffness. The need for suitable polymer biocomposites used for load-bearing bone defect is immediate and increasing. Compared to polyamide66 (PA66), polyamide46 (PA46) shows better mechanical properties and dimensional stability for its higher crystallinity and higher degree of molecular regularity [8]. Therefore, due to the successful application of the HA/PA66 composite and the better mechanical properties of the PA46, HA/PA46 composite is studied as biomaterial in the present study.

Furthermore, fibers are widely used for improving the mechanical performance of polymer composite nowadays [9–13], such as carbon, glass and aramid fibers. Carbon fibers (CF) have been widely used as reinforcements for ceramic, polymeric matrices in light of their excellent properties including light weight, high strength and modulus, good electrical conductivity and stability at elevated temperatures [14,15]. Moreover, many studies indicate that carbon fibers exhibit biocompatibility both *in vitro* and *in vivo* [16–19], and have already been used as biomaterial [20–22].

Taken together, to combine the advantages of the abovementioned various components, we prepared a novel biocomposite–carbon fiber-reinforced nano-hydroxyapatite/polyamide66 composite (CF/HA/PA46) by an extrusion technique in this study. Then the mechanical performances and the preliminary biocompatibility of the CF/HA/PA46 were characterized.

Material and Methods

Fabrication of CF reinforced HA/PA46 biocomposites

HA/PA46 composites were prepared by the following procedure: HA/PA46 (25: 75, mass fraction) composites were prepared in N,N-dimethyl acetamide (DMAC) solution by co-deposition method. PA46 (BASF) and DMAC were added into the three-neck flask, then the temperature was increased to 140°C, and keeping the temperature at 140°C for 4h till PA46 was dissolved completely, thus the co-solution of PA46 and DMAC was obtained, HA powder (Sichuan Guona Technology Co., Ltd., China) was added into the co-solution, stirring 2 h. When the reaction ended, the co-precipitation mixture was cooled down to room temperature. After fully washed by deionized water 4 times and ethanol twice, the obtained HA/PA46 composite products were dried in a vacuum oven at 80–85°C for 48h.

CF/HA/PA46 composites containing 5, 10, 15 and 20 wt% CF (Beijing Boyu high-tech new material technology Co., Ltd., China) were prepared with a twin-screw extruder (TSE-30A, Ruiya Polymer Processing Equipment Co., Ltd., China, screw diameter 32mm) by extrusion compounding method. The extrusion temperature was ranged from 250 to 290°C, main engine speed was 50 Hz and feed rate was 40 Hz. The obtained biocomposites with different CF contents were named as 5CF/HA/PA46, 10CF/HA/PA46, 15CF/HA/PA46, and 20CF/HA/PA46, respectively.

The specimens for mechanical properties testing were prepared using injection molding craft with an injection molding machine (SI-100IV-F200B, Toyo Machinery & Metal Co. Ltd, Japan). The injection temperature was ranged from 270 to 310°C under 90 MPa.

FT-IR, XRD, and SEM analysis

Fourier transform infrared absorption spectra (FT-IR, Nicolet 170SX, USA) was used to determine the chemical bonding between CF, HA and PA46 of the 20CF/HA/PA46 biocomposite powders. The composition and crystallinity of the 20CF/HA/PA46 biocomposite was detected by X-ray diffraction (XRD, X'Pert Pro MPD, Philips, Netherlands). The surface morphology and distribution of CF in 20CF/HA/PA46 biocomposite were observed by SEM (JEOL JSM5600LV, Japan).

Mechanical properties

The bending strength, tensile strength and tensile modulus of the CF/HA/PA46 biocomposites samples were conducted by a mechanical testing machine (REGER 30-50, Shenzhen Reger Co., Ltd., China) with 50 kN load cells at a cross-head speed of

5 mm/min. For each test, 5 replicates samples were conducted and the results were expressed as the Mean \pm SD.

Cell culture and morphology

In this study, MG-63 cells were used to evaluate the cytocompatibility of 20CF/HA/PA46 biocomposite, which had previously been widely employed as *in vitro* test for assessing the cytocompatibility of many types of biomaterials [23,24]. MG-63 cells were cultured in Dulbecco's Modified Eagle's Medium (DMEM, Gibco, USA), supplemented with 100 U/mL of penicillin, 100 μ g/mL of streptomycin, and 10% fetal bovine serum (FBS, Gibco, USA), and cultured in 25 mL culture bottles in a humidified 5% CO₂ atmosphere at 37°C. The culture medium was refreshed every 2 days.

The 20CF/HA/PA46 samples with a size of Φ 8 \times 2 mm were fabricated, and the HA/PA composites with the same size were made and used as control. MG-63 cells were seeded onto the samples inside a 24-well plate with an initial density of 1×10^4 cells/well. After 3 days of culture, cells were fixed with 4% paraformaldehyde in PBS solution for 15 min, followed by washing with PBS solution and permeabilized at 4°C for 5 min. They were then incubated with 1% bovine serum albumin (BSA)/PBS solution at 37°C for 5 min to block non-specific binding. FITC-conjugated phalloidin (Millipore) (1: 1000 in 1% BSA/PBS) was then added at 37°C for 1 h. After washing for 3 times with 1 \times PBS solution for 5min, DAPI (1: 1000 in 1 \times PBS buffer at pH 8.0) was added at 25°C for 8 min. The samples were then given a final wash (15 min \times 3) before mounting under Vectashield antifade mountants, and observed under a fluorescence microscope (Leica, Germany).

Cell viability

To analyze cytocompatibility of 20CF/HA/PA46 biocomposite, cell proliferation on 20CF/HA/PA46 biocomposite was studied. The initial cell adhesion to material surface and the subsequent cell proliferation on the material showed the quantitative indirect data on material properties, which could be used for evaluation of living cells compatibility with the examined biocomposite: the biochemical reactivity of the biocomposite, the release of toxic products from the biocomposite, the biophysical surface properties (such as topography, chemistry, wettability) of the material etc [24–26]. Hence, the cell viability test for *in vitro* cell adhesion and proliferation on biocomposite is widely used to evaluate its cytocompatibility. In our study, the cell viability was investigated by 4,5-dimethylthiazol-2-yl-2,5-diphenyl tetrazolium bromide (MTT) colorimetric assay following culture periods of 1, 3, 5, and 7 days. In the MTT assay, the mitochondrial dehydrogenases of viable cells cleaved the tetrazolium ring of the substrate to yield purple formazan crystals. The resulting purple solution was

spectrophotometrically measured at 570 nm using a Bio Assay Reader (HTS7000 plus, Perkin Elmer, USA), and the relative intensities were plotted.

Alkaline phosphatase activity

Alkaline phosphatase (ALP) activity is one of the most widely used markers for the early osteodifferentiation of osteoblasts. After culture periods of 1, 3, 5 and 7 days, ALP activity was measured to evaluate the normal osteoblast phenotypic responses to 20CF/HA/PA46 biocomposite. Adhered cells on the biocomposite were lysed with 0.05% Triton X-100 (Amresco, USA) to release intracellular ALP. The lysed solution was incubated with 500 μ L of ALP substrate solution for 30 min at 37°C. The reaction was terminated by the addition of 250 μ L of 0.2 mol/L NaOH. A colorimetric assay was used to measure the absorbance of the solution at 405 nm. The total protein concentration of the samples was then evaluated with a bicinchoninic acid (BCA) protein assay kit (Thermo, USA), and the absorbance in each sample was normalized based on the protein content.

Gene expression level by quantitative real-time PCR

To further evaluate whether osteoblast differentiation was affected by 20CF/HA/PA46 biocomposite, we analyzed the expression levels of several marker genes for osteoblast differentiation by quantitative real-time PCR (qPCR). In order to induce cell differentiation, MG-63 cells on all test substrates were cultured in osteogenic media [DMEM containing 10% FBS, 2.1 mM Na- β -glycerol phosphate, and 50 μ g/ml ascorbic acid (Sigma-Aldrich, USA)]. The culture medium was refreshed every 3 days.

Briefly, the total RNA in MG-63 cells (n=7) for each group was extracted at 7 day using TRIzol[®] reagent (Invitrogen, USA). Then 1 μ g RNA from each sample was reverse transcribed into complementary DNA (cDNA) using PrimeScript[™] RT reagent kit (Takara, Japan). The expression levels of type I collagen (Col-I, early phase), ALP (mid phase) and osteocalcin (OCN, late phase) were examined by a CFX Connect[™] Real-time PCR detection system (Bio-Rad Laboratories Inc., USA) with the SYBR Green Master Mix (Roche, Switzerland). The relative expression levels of the target genes were normalized to the expression of the housekeeping gene glyceraldehyde-3-phosphate dehydrogenase (GAPDH). The primer sequences were listed in Table 1. All qPCR analyses were repeated independently 3 times.

Statistical analysis

The results were expressed as the Means \pm SD. Statistical analysis was performed by one-way analysis of variance (ANOVA) followed by the Student-Newman-Keuls post-test using SPSS 20.0 statistical software. The level of statistical significance was defined as $P<0.05$.

Table 1. Primer sequences used in the present study.

Target gene	Primer sequence (5'-3')
GAPDH	Forward: GGCATTGCTCTCAATGACAA
	Reverse: TGTGAGGGAGATGCTCAGTG
ALP	Forward: AGGGCTGTAAGGACATCGCCTACCA
	Reverse: GACTGCGCCTGGTAGTTGTTGTGAG
Col-I	Forward: CCAGAAGAAGTGGTACATCAGCAA
	Reverse: CGCCATACTCGAACTGGAATC
OCN	Forward: CCTCACACTCTCGCCCTATTGG
	Reverse: GCTCACACACCTCCCTCTGG

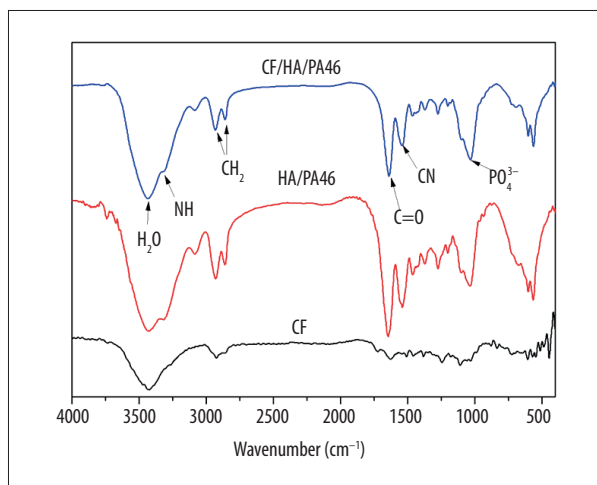


Figure 1. The FT-IR spectra of CF/HA/PA46 ternary composite, HA/PA46 and CF.

Results

FT-IR analysis

The FT-IR spectra of CF, HA/PA46 and 20CF/HA/PA46 were shown in Figure 1. The nitrogen-hydrogen (NH) stretching vibrational peak of PA46 was at the band of 3301 cm^{-1} , and the carbon hydrogen (CH_2) vibrational peaks of the main molecule chain of PA46 were at the bands of 2939 cm^{-1} and 2862 cm^{-1} . The characteristic peaks of stretching vibration of carbon-nitrogen (CN) and the carbonyl vibration (C=O) peaks were at 1537 cm^{-1} and 1634 cm^{-1} , respectively. The peak at 3400–3600 cm^{-1} was attributed to H_2O , and this peak overlapped the peaks of the hydroxyl (OH) of HA (in general, the peak was at about 3567–3572 cm^{-1} [27]). It was clear that the HA and PA46 peaks were found in 20CF/HA/PA46 biocomposite. In addition, compared to HA/PA46, no new peaks and manifest peaks shift were observed in 20CF/HA/PA46 biocomposite.

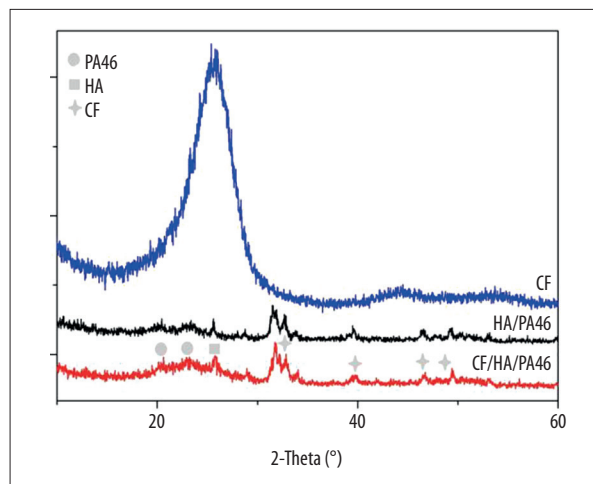


Figure 2. The XRD pattern of CF/HA/PA46, HA/PA46 and CF.

XRD analysis

The XRD patterns of CF, HA/PA46, and 20CF/HA/PA46 composite were shown in Figure 2. In the patterns, the 2 peaks at $2\theta=20.4^\circ$ and 23.0° on the 20CF/HA/PA46 spectra were belonged to the characteristic diffraction of PA46. The characteristic peaks of HA appeared at $2\theta=25.7^\circ$, 31.7° , and 33.9° in the 20CF/HA/PA46 composite, $2\theta=25.7^\circ$ was also the characteristic peak of CF. The results revealed that all the characteristic peaks of PA46, HA and CF existed in the 20CF/HA/PA46 composite, and there was no appearance of new peaks.

SEM observation

As shown in Figure 3, the surface morphology of 20CF/HA/PA46, 15CF/HA/PA46 and HA/PA46 were observed by SEM. It was obvious that the irregular and basin-shaped surface of the fracture formed in CF/HA/PA46 biocomposite, which were considered to be the characteristic of toughness, while relatively regular surface (as shown in Figure 3E) of fracture formed in HA/PA46 composite. A uniformed distribution with random orientations of CF was observed in the HA/PA46 matrix. In addition, there was no clear evidence of cracks and debonding between CF and HA/PA46 matrix.

Mechanical properties

The mechanical strength and modulus of the CF/HA/PA46 biocomposites were shown in Table 2. It was clear that the strength of biocomposite was closely correlated with the content of CF, with the bending strength of 159–223 MPa and tensile strength of 127–199 MPa. Obviously, higher CF content resulted in higher bending strength when the CF content was in the range of 0–20%. However, when the CF content arrived at 20%, the tensile strength was 185 MPa, a little bit lower than that of 15CF/HA/PA46. The values of tensile modulus of 5CF/HA/PA46, 10CF/

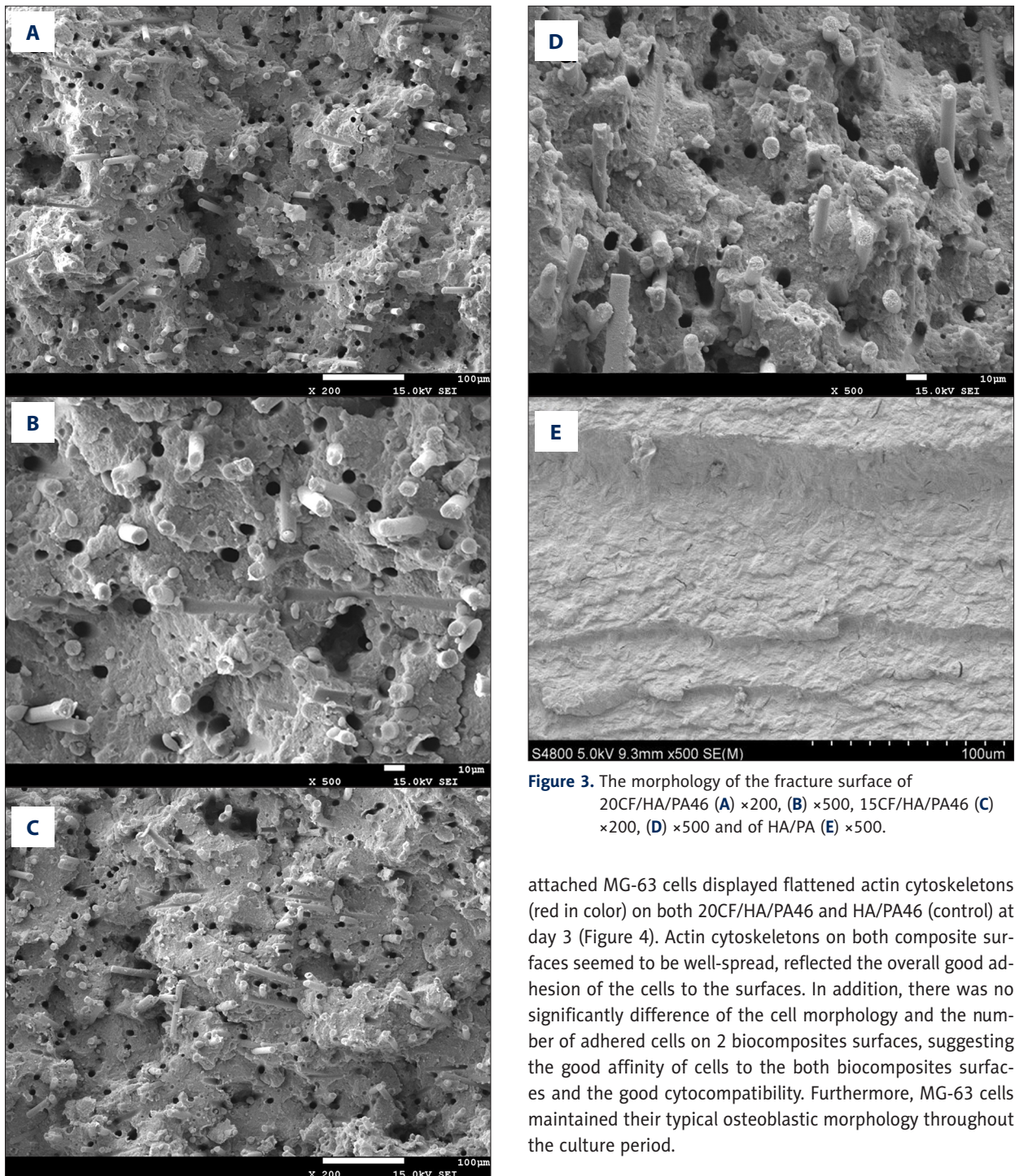


Figure 3. The morphology of the fracture surface of 20CF/HA/PA46 (A) $\times 200$, (B) $\times 500$, 15CF/HA/PA46 (C) $\times 200$, (D) $\times 500$ and of HA/PA46 (E) $\times 500$.

attached MG-63 cells displayed flattened actin cytoskeletons (red in color) on both 20CF/HA/PA46 and HA/PA46 (control) at day 3 (Figure 4). Actin cytoskeletons on both composite surfaces seemed to be well-spread, reflected the overall good adhesion of the cells to the surfaces. In addition, there was no significant difference of the cell morphology and the number of adhered cells on 2 biocomposites surfaces, suggesting the good affinity of cells to the both biocomposites surfaces and the good cytocompatibility. Furthermore, MG-63 cells maintained their typical osteoblastic morphology throughout the culture period.

Cell viability

As shown in Figure 5, the optical density values increased significantly over time, and there was no significant difference between the biocomposite and control at days 1, 3, 5 and 7 ($P > 0.05$). That is, the MG-63 cells were viable and exhibited good cell proliferation and positive cellular responses to both the 20CF/HA/PA46 biocomposite and control.

HA/PA46, 15CF/HA/PA46, and 20CF/HA/PA46 samples were 7.7 GPa, 8.5 GPa, 9.0 GPa, and 10.8 GPa, respectively.

Cell morphology

The distribution of cytoskeletal F-actin was analyzed by immunofluorescence staining. The results revealed that the

Table 2. The mechanical properties of CF/HA/PA46 composites.

Samples	Bending strength (MPa)	Tensile strength (MPa)	Tensile modulus (GPa)
HA/PA46	116±3	95±7	4.6±0.4
5 CF/HA/PA46	159±7	127±8	7.7±0.6
10 CF/HA/PA46	181±4	163±6	8.5±0.6
15 CF/HA/PA46	223±9	199±5	9.0±0.4
20 CF/HA/PA46	222±6	185±5	10.8±0.5

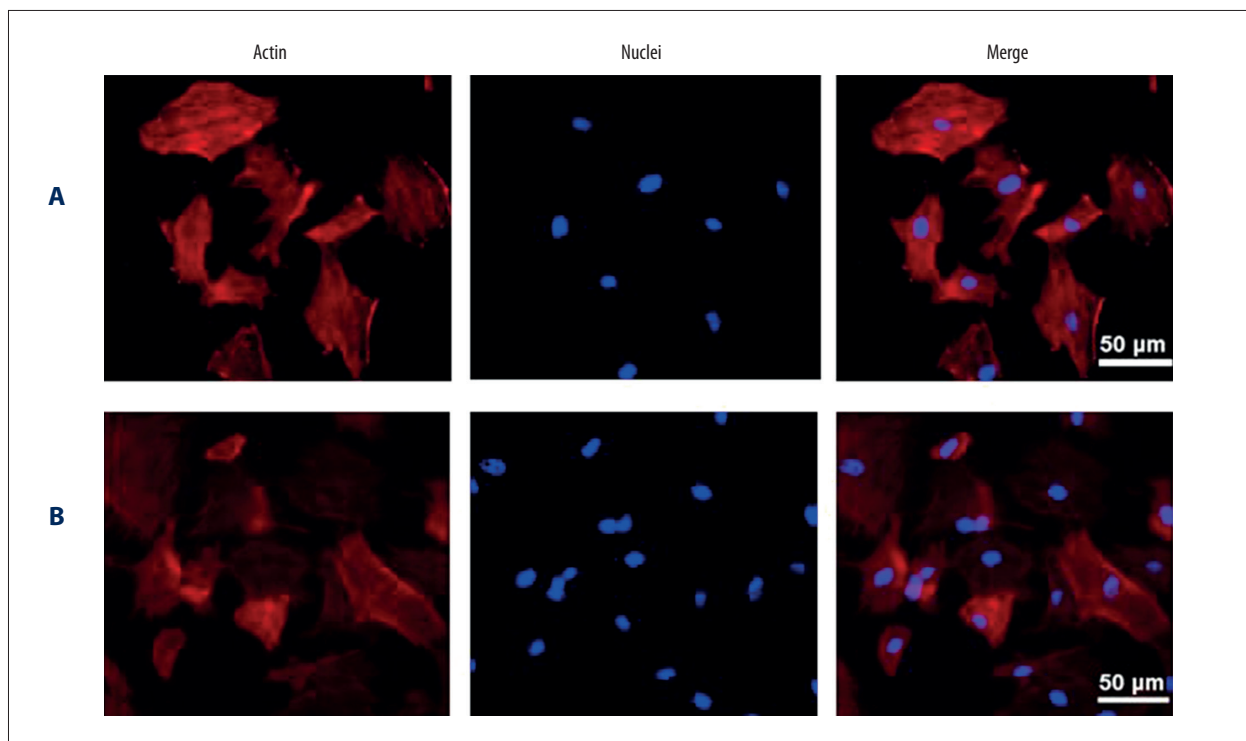


Figure 4. Images of MG-63 cells on the CF/HA/PA46 (A) and HA/PA46 (B) composite at day 3. “Merge” represents the merged images of actin cytoskeletons (stained red) and nuclei (stained blue).

ALP activity

The ALP activity of MG-63 cells cultured on the 20CF/HA/PA46 biocomposite and control was detected on days 1, 3, 5 and 7 (Figure 6). The ALP activity of the MG-63 cells on all samples increased with increasing time of culture. Moreover, there was no significant difference between the 20CF/HA/PA46 and control at all the experimental time, confirmed by the statistical analysis ($P>0.05$).

The expression levels of osteogenic marker genes

The data showed that the mRNA levels of Col-I, ALP and OCN was nearly the same on 20CF/HA/PA46 and HA/PA46 control surfaces after 7 days (Figure 7). There was no significant difference ($P>0.05$). The results suggested that 20CF/HA/

PA46 biocomposite had no negative effects on osteoblast differentiation.

Discussion

In general, metal materials as biomaterial, exhibiting good mechanical properties such as strength, toughness and flexibility, can provide sufficient mechanical support. Hence, they are good candidates for bone repair in load-bearing sites. However, in the majority of clinical cases, those metal devices have to be removed by a second operation because of the mismatch property of the metal materials with high modulus. This mismatch is considered to be a key factor leading to stress shielding and localized osteopenia under and near the devices, and therefore hamper the bone healing process [12]. Hence, the

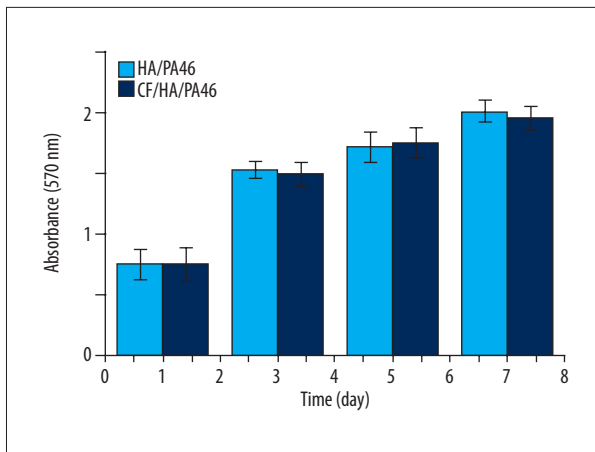


Figure 5. Viability of MG-63 cells on ternary composites by MTT assays at 1, 3, 5 and 7 days.

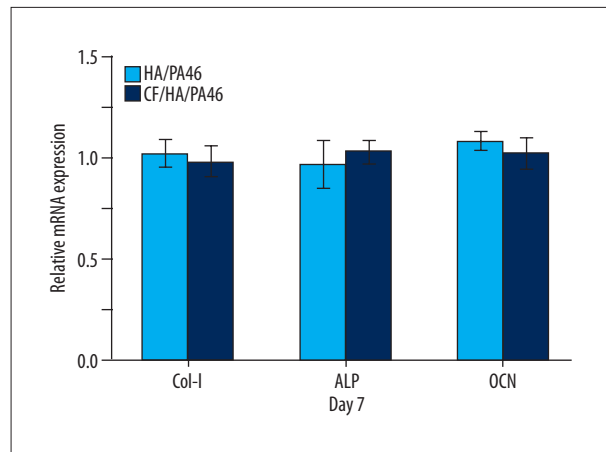


Figure 7. The relative expression levels of Col-I, ALP and OCN in MG-63 cells cultured on ternary composites after 7 days.

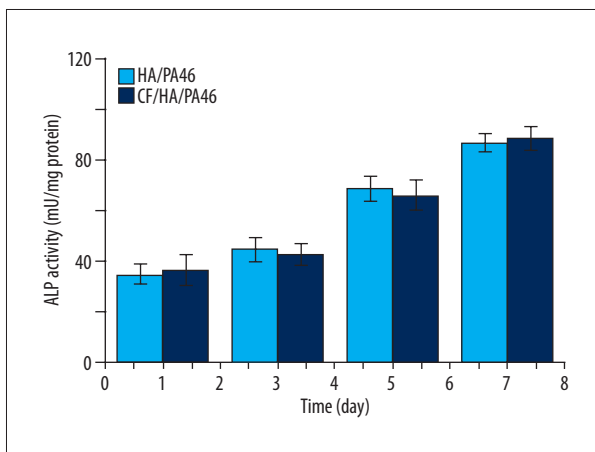


Figure 6. ALP activity of MG-63 cells on ternary composites after 1, 3, 5 and 7 days of culture.

need for novel materials with favorable mechanical properties for load-bearing defect repair is imperative and urgent in clinical practice. Recently, more and more researches are focused on such development of new materials. Fiber-reinforced materials, a common approach to obtain improved strength and modulus of polymer composite, are widely reported [27,28]. Recently, a glass-fiber-reinforced HA/PA66 composite (GF/HA/PA66) was prepared, and the results confirmed that the mechanical properties can be greatly improved by the reinforcement of GF [12,29]. The positive results encouraged us to develop a novel fiber-reinforced HA/PA composite to increase its mechanical performances. Besides, PA46 was found to exhibit superior mechanical properties than those of PA66, including higher stiffness, higher fatigue resistance, higher thermal stability and good processability, owing to its high amide content per repeating unit and its symmetrical chain structure [8]. Whereas, the HA/PA46 composites have been rarely reported. Taken together, a novel biocomposite CF/HA/PA46 was developed by addition of CF into HA/PA46 in the present study.

In HA/PA46 matrix, no CF aggregation and no preferred orientation were found by SEM, suggesting that there was a random and evenly distribution of CF in the matrix. Moreover, CF was tightly bonded to the HA/PA46 matrix and there were no cracks between the CF and matrix, which could be considered to be a well adhesion between CF and HA/PA46 matrix [29–31]. No morphology changes of HA/PA46 matrix were observed by SEM. There were some cavities and irregular basin-shaped fracture surface formed, indicating that the addition of CF had manifestly improved the toughness of biocomposite, compared to HA/PA46 matrix.

Furthermore, the mechanical properties of the CF/HA/PA46 were tested to evaluate the effects of the addition of CF into HA/PA46 matrix. The resultant composite showed a tensile strength of 127–199 MPa and a bending strength of 159–223 MPa, and a modulus of 7.7–10.8 GPa, respectively. Obviously, the test values varied with the CF contents, indicating that CF could improve the mechanical properties of the HA/PA46 composite effectively. Moreover, among those samples, 15CF/HA/PA46 had suitable bending and tensile strength and its modulus was very close to that of natural bone [32]. Hence, the CF/HA/PA46 biocomposite has great potential for bone repair in load-bearing sites.

Biocompatibility is also very crucial for biocomposite. To evaluate the influences of the CF addition into HA/PA46, the MG-63 cells were co-cultured with the CF/HA/PA46 biocomposite and the control (HA/PA46). Cell adhesion on materials are considered to be the first phase of the cell-material interaction and play a key role in the following cell behaviors, including the cell morphology, proliferation, and differentiation on materials [33]. In our present study, the cell viability of MG-63 cells was evaluated by a MTT assay. The OD value increased over time in both CF/HA/PA46 biocomposite samples and HA/

PA46 controls, and there were no significant differences at days 1, 3, 5, and 7 ($P>0.05$), indicating that both CF/HA/PA46 and HA/PA46 were in favor of cell viability and proliferation. Furthermore, the results were also supported by the immunofluorescence microscopy observation results. It was found that the actin cytoskeletons on both composite surfaces were well-spread and the amount of the cells adhered to 20CF/HA/PA46 and to HA/PA were similar after 3-day culture. Obviously, the CF/HA/PA46 biocomposite showed favorable effects on cell morphology and viability.

ALP is a traditional marker of osteoblast differentiation and is related to the production of a mineralized osteoblast [34,35]. In the present study, the ALP activity of MG-63 cells on 20CF/HA/PA46 and HA/PA increased over time during the experimental period. The biocomposite and control showed no significant differences in ALP expression level on days 1, 3, 5 and 7, indicating that the 20CF/HA/PA46 biocomposite was suitable for the differentiation of MG-63 cells.

Besides, the addition of CF exhibited no negative effect on Col-I (early phase), ALP (mid phase) and OCN (late phase) mRNA

expression of MG-63 cells on the 20CF/HA/PA46 by qPCR analysis. These results to some extent were in accordance with those of recent and related reports, as it had been shown that HA/PA composite has a positive effect on osteoblast adhesion, viability, and differentiation, thus influencing the bone cell responses as it comes in contact with HA/PA substrate [36–39].

Conclusions

A novel biocomposite for load-bearing defect repair was prepared by using CF reinforcement to HA/PA46 in this study. The CF showed good compatibility to matrix and tightly bonded to matrix. The addition of CF into HA/PA46 significantly improved the mechanical performances of the CF/HA/PA46 biocomposite. The resultant biocomposite had similar modulus to natural bone, and even better strength than natural bone. Moreover, the addition of CF showed favorable effects on the cell adhesion, proliferation and differentiation, exhibited good cytocompatibility. In conclusion, the obtained CF/HA/PA46 composite, with good mechanical performances and cytocompatibility, has high potential for bone repair in load-bearing sites.

References:

- Huiskes R, Weinans H, Van Rietbergen B: The relationship between stress shielding and bone resorption around total hipstems and the effects of flexible materials. *Clin Orthop Relat R*, 1992; 274: 124–34
- Kanayama M, Cunningham BW, Haggerty CJ et al: *In vitro* biomechanical investigation of the stability and stress-shielding effect of lumbar interbody fusion devices. *J Neurosurg*, 2000; 93: 259–65
- Jung HD, Kim HE, Koh YH: Production and evaluation of porous titanium scaffolds with 3-dimensional periodic macrochannels coated with micro-porous TiO₂ layer. *Materials Chemistry and Physics*, 2012; 135: 897–902
- Wei J, Li Y: Tissue engineering scaffold material of nano-apatite crystals and polyamide composite. *Eur Polym J*, 2004; 40(3): 509–15
- Ou Y, Jiang D, Quan Z et al: Application of artificial vertebral Body of biomimetic nano-Hydroxyapatite/Polyamide 66 composite in anterior surgical treatment of thoracolumbar fractures. *Zhongguo Xiu Fu Chong Jian Wai Ke Za Zhi*, 2007; 21(10): 1084–88
- Zhao Z, Jiang D, Ou Y et al: A hollow cylindrical nano-hydroxyapatite/polyamide composite strut for cervical reconstruction after cervical corpectomy. *J Clin Neurosci*, 2012; 19(4): 536–40
- Yang X, Song Y, Liu Li et al: Anterior reconstruction with nanohydroxyapatite/polyamide-66 cage after thoracic and lumbar corpectomy. *Orthopedics*, 2012; 35(1): 66–73
- Chiu F-C, Huang I-N: Phase morphology and enhanced thermal/mechanical properties of polyamide 46/graphene oxide nanocomposites. *Polym Test*, 2012; 31(7): 953–62
- Campbell M, Bureau MN, Yahia L: Performance of CF/PA12 composite femoral stems. *J Mater Sci-Mater M*, 2008; 19(2): 683–93
- Lee Y, Porter RS: Crystallization of Poly(Etheretherketone) (PEEK) in carbon fibre composites. *Polym Eng Sci*, 1986; 26(9): 633–39
- Steinberg EL, Rath E, Schlaifer A et al: Carbon fibre reinforced PEEK Optima – a composite material biomechanical properties and wear/debris characteristics of CF-PEEK composites for orthopedic trauma implants. *J Mech Behav Biomed*, 2013; 17: 221–28
- Su B, Peng X, Jiang D et al: *In vitro* and *in vivo* evaluations of nano-hydroxyapatite/polyamide66/glass fibre (n-HA/PA66/GF) as a novel bioactive bone screw. *PLoS One*, 2013; 8(7): e68342
- Gunilla M, Ostberg K, Seferis JC: Annealing effects on the crystallinity of polyetheretherketone (PEEK) and its carbon fibre composite. *J Appl Polym Sci*, 1987; 33(1): 29–39
- Soutis C: Fibre reinforced composites in aircraft construction. *Prog Aerosp Sci*, 2005; 41: 143–51
- Faultsch de Paiva JM, dos Santos ADN, Dosreze MC et al: Mechanical and morphological characterizations of carbon fibre fabric reinforced epoxy composites used in aeronautical field. *Mater Res*, 2009; 12(3): 367–74
- Wang H, Li Y, ZuoY et al: Biocompatibility and osteogenesis of biomimetic nano-hydroxyapatite/polyamide composite scaffolds for bone tissue engineering. *Biomaterials*, 2007; 28(22): 3338–48
- Rajzer I, Kwiatkowski R, Piekarczyk W et al: Carbon nanofibres produced from modified electrospun PAN/hydroxyapatite precursors as scaffolds for bone tissue engineering. *Mat Sci Eng: C*, 2012; 32(8): 2562–69
- Cieřlik M, Mertas A, Morawska-Chochól A et al: The evaluation of the possibilities of using PLGA co-polymer and its composites with carbon fibres or hydroxyapatite in the bonetissue regeneration process – *in vitro* and *in vivo* examinations. *Int J Mol Sci*, 2009; 10(7): 3224–34
- Cheng Q, Rutledge K, Jabbarzadeh E: Carbon nanotube-Poly (lactide-co-glycolide) composite scaffolds for bone tissue engineering applications. *Ann Biomed Eng*, 2013; 41(5): 904–16
- Ernstberger T, Buchhorn G, Heidrich G: Magnetic resonance imaging evaluation of intervertebral test spacers: An experimental comparison of magnesium versus titanium and carbon fibre reinforced polymers as biomaterials. *Irish J Med Sci*, 2010; 179(1): 107–11
- Shen L, Yang H, Ying J et al: Preparation and mechanical properties of carbon fibre reinforced hydroxyapatite/poly(lactide)biocomposites. *J Mater Sci Mater Med*, 2009; 20(11): 2259–65
- Saito N, Aoki K, Usui Y et al: Application of carbon fibres to biomaterials: A new era of nano-level control of carbon fibres after 30-years of development. *Chem Soc Rev*, 2011; 40(17): 3824–34
- Graziano A, d'Aquino R, Cusella-De Angelis MG et al: Scaffold's surface geometry significantly affects human stem cell bone tissue engineering. *J Cell Physiol*, 2008; 214(1): 166–72
- Deng Z, Yin B, Li W et al: Surface characteristics of and *in vitro* behavior of osteoblast-like cells on titanium with nanopography prepared by high-energy shot peening. *Int J Nanomedicine*, 2014; 28(9): 5565–73

25. Bonartsev AP, Yakovlev SG, Zharkova II et al: Cell attachment on poly(3-hydroxybutyrate)-poly(ethylene glycol) copolymer produced by *Azotobacter chroococcum* 7B. *BMC Biochem*, 2013; 14: 12
26. Zheng Z, Bei F, Tian H et al: Effects of crystallization of polyhydroxyalkanoate blend on surface physicochemical properties and interactions with rabbit articular cartilage chondrocytes. *Biomaterials*, 2005; 26(17): 3537-48
27. Chen S, Lei M, Xie X et al: PLGA/TCP composite scaffold incorporating bioactive phytomolecule caritin for enhancement of bone defect repair in rabbits. *Acta Biomaterialia*, 2013; 9(5): 6711-22
28. Zhang X, Lu M, Wang Y et al: The development of biomimetic spherical hydroxyapatite/polyamide66 biocomposites as bone repair materials. *Int J Polym Sci*, 2014; 2014: 579252
29. Kurtz SM, Devine JN: PEEK biomaterials in trauma, orthopedic, and spinal implants. *Biomaterials*, 2007; 28(32): 4845-69
30. Rong M, Zhang M, Liu Y et al: The effect of fibre treatment on the mechanical properties of unidirectional sisal-reinforced epoxy composites. *Compos Sci Technol*, 2001; 61(10): 1437-47
31. Qiao B, Li J, Zhu Q et al: Bone plate composed of a ternary nanohydroxyapatite/polyamide-46/glass fibre composite: Biomechanical properties and biocompatibility. *Int J Nanomedicine*, 2014; 9(1): 1423-32
32. Rho JY, Kuhn-Spearing L, Zioupos P: Mechanical properties and the hierarchical structure of bone. *Med Eng Phys*, 1998; 20(2): 92-102
33. Li H, Gong M, Yang A et al: Degradable biocomposite of nano calcium-deficient hydroxyapatite-multi(amino acid) copolymer. *Int J Nanomedicine*, 2012; 7: 1287-95
34. Lao L, Wang Y, Zhu Y et al: Poly (lactide-co-glycolide)/hydroxy-apatite nanofibrous scaffolds fabricated by electrospinning for bone tissue engineering. *J Mater Sci Mater Med*, 2011; 22(8): 1873-84
35. Zhang X, Zhang Y, Zhang X et al: Mechanical properties and cytocompatibility of carbon fibre reinforced nano-hydroxyapatite/polyamide66 ternary biocomposite. *Mech Behav Biomed Mater*, 2015; 42: 267-73
36. Akay C, Yalug S: Biomechanical 3-dimensional finite element analysis of obturator protheses retained with zygomatic and dental implants in maxillary defects. *Med Sci Monit*, 2015; 21: 604-11
37. Jiao Y, Ma S, Wang Y et al: Epigallocatechin-3-gallate reduces cytotoxic effects caused by dental monomers: A hypothesis. *Med Sci Monit*, 2015; 21: 3197-202
38. Li H, Chen F, Wang Z et al: Comparison of clinical efficacy between modular cementless stem protheses and coated cementless long-stem protheses on bone defect in hip revision arthroplasty. *Med Sci Monit*, 2016; 22: 670-77
39. Timothy J, Wilson J, Rice E et al: Nanocrystalline hydroxyapatite intervertebral cages induce fusion after anterior cervical discectomy and may be a safe alternative to PEEK or carbon fiber intervertebral cages. *Br J Neurosurg*, 2016; 30(6): 654-57